Neutron Capture Resonances in ^{116}Sn, ^{118}Sn, and ^{120}Sn

K. Wisshak, F. Voss, F. Käppeler
Institut für Kernphysik

FORSCHUNGSZENTRUM KARLSRUHE

Technik und Umwelt

Wissenschaftliche Berichte

FZKA 5755

NEUTRON CAPTURE RESONANCES IN
^{116}Sn, ^{118}Sn, AND ^{120}Sn

K. WISSHAK, F. VOSS, and F. KÄPPELER

Institut für Kernphysik

ABSTRACT

The neutron capture cross sections of ^{116}Sn, ^{118}Sn, and ^{120}Sn which were determined recently with the Karlsruhe 4π BaF$_2$ detector have been reanalyzed at low energies. Resonance parameters were extracted by means of a shape analysis program, thus allowing a more reliable determination of the averaged cross sections below 20 keV. This study confirms the previously reported stellar cross sections. Accordingly, the results of the s–process studies based on these data remain unchanged.

ZUSAMMENFASSUNG

NEUTRONENEINFANGRESONANZEN
IN ^{116}Sn, ^{118}Sn UND ^{120}Sn

Die kürzlich mit dem Karlsruher 4π BaF$_2$ Detektor gemessenen Neutroneneinfang-querschnitte von ^{116}Sn, ^{118}Sn und ^{120}Sn wurden bei niedrigen Energien neu ausgewertet. Mit einem Analyseprogramm wurden Resonanzparameter ermittelt, die eine genauere Bestimmung der Querschnitte unterhalb von 20 keV ermöglichen. Die neuen Ergebnisse bestätigen die früher veröffentlichten stellaren Querschnitte. Daher bleiben die Untersuchungen zum s–Prozess, die auf diesen Daten basieren, unverändert gültig.

1 INTRODUCTION

The origin of the stable isotopes in the Cd–In–Sn region is characterized by a complex mixture of contributions from the s, r, and p process of nucleosynthesis, and is presently not well understood. The rather complicated abundance pattern results partly from the influence of the numerous isomers on the reaction flow, which can be populated in the s process and the r process as well. Hence, both processes may contribute to the solar abundances of the rare isotopes ^{113}In, ^{114}Sn, and ^{115}Sn in addition to the contributions from the p process [1, 2].

In an attempt to improve the experimental data for the s–process contribution the stellar neutron capture cross sections of the tin isotopes were measured with the Karlsruhe 4π BaF$_2$ detector for registration of capture events [3]. Compared to earlier results, a five times better accuracy could be achieved for the stellar cross sections at kT=30 keV, and, for the first time, reliable values were also obtained at lower temperatures. With these data the s–process abundances of the tin isotopes could be described quantitatively.

In this investigation, the differential capture cross sections of ^{116}Sn, ^{118}Sn, and ^{120}Sn were measured with sufficient resolution that single resonances could be resolved up to about 20 keV neutron energy. Despite of this feature, the stellar cross sections were only determined by averaging the observed capture yield [3]. This simplification may be justified to good approximation according to a similar study on ^{134}Ba [4]. On the other hand, there could still be doubts on the results at low neutron energies, where a significant background due to capture of scattered neutrons had to be subtracted in the original data. Therefore, these data have been reanalysed by means of a shape analysis program for determining the resonance parameters. From these parameters new and more reliable values for the low energy part of the stellar cross sections were derived, an improvement that is especially important since stellar model calculations indicate that most of the s process takes place at thermal energies of 12 keV of even less [5, 6].

2 Experiment and data evaluation

Experiment and data analysis have been described in detail in Ref.[3]. Continuous neutron spectra were produced via the ^{7}Li(p,n)^{7}Be reaction using the pulsed proton beam of the Karlsruhe 3.75 MV Van de Graaff accelerator. Capture events were registered with the Karlsruhe 4π BaF$_2$ detector [7] with a time resolution of about 1 ns. The metallic samples with isotopic enrichments between 97.6 % and 99.6 % were located at a neutron flight path of 78 cm. The sample masses were 4.7 to 10.3 g but for ^{116}Sn a second thinner sample

of 2.4 g was used as well. Three runs were performed with different maximum neutron energies. All spectra could be analysed down to a minimum energy of 3 keV.

After summation of the capture yields from all three runs the resulting time–of–flight (TOF) spectra were analysed with the FANAC code [8] in the same way as described for ^{134}Ba [4]. The global input parameters like strength functions or nuclear radii were the same as in the calculations of the multiple scattering and self–shielding corrections described in Ref.[3]. Known neutron widths of s– and p–wave resonances as well as resonance spins were adopted from literature [9].

The TOF measurement of the neutron energy is determined by the pulse width of the proton beam (0.7 ns), the time resolution of the 4π BaF$_2$ detector (0.5 ns), and by the sample thickness (1.8 – 3.7 mm) resulting in an average resolution in neutron energy of ±55 eV at 10 keV, ±35 eV at 7 keV and ±23 eV at 5 keV. Thus, the shape of all resonances is completely determined by the experimental resolution which means that it was not possible to derive the individual resonance parameters Γ_n or Γ_γ directly from the present experiment. Instead, the resonance area $A_\gamma = g\Gamma_n\Gamma_\gamma/(\Gamma_n + \Gamma_\gamma)$ was determined in the fits.

If no information on Γ_n is available the average neutron width can be calculated via the relation [10]

$$g_J < \Gamma_n >_{lJ} = \nu_{lJ} g_J D_J S_l \sqrt{E} v_l(E) \qquad (1)$$

where the quantities g, D, S, ν, and v_l denote the statistical weight factor, the mean level spacing, the strength function, the number of possible channel spins, and the penetrability factor. For p–wave resonances, this expression reduces to

$$g < \Gamma_n >_1 = D_s S_1 \sqrt{E} \frac{(kR)^2}{1 + (kR)^2}. \qquad (2)$$

All p–wave resonances were analysed for the two possible values of the statistical weight factor g $=3/2$ and $1/2$, and the average was adopted as the final result if no other information on g was available.

The reliability of the resonance areas A_γ depends on the available experimental information on neutron widths and spins. This is quite different for the three isotopes and needs to be discussed separately.

- ^{120}Sn: For this isotope a nearly complete set of Γ_n values and orbital angular momenta l is available from the work of Carlton et al. [9, 11]. Fig 1 shows a comparison for g$< \Gamma_n >$ averaged over three energy bins between the data of Ref.[9] and the values calculated according to Eq.(2). The good agreement justifies to use the calculated values for those resonances which were found in the present work for the first time. These values have to be considered as upper limits, since the corresponding resonances would have been discovered in the total cross section measurements of Ref.[11] otherwise. In total, a set of 55 resonances was analysed and compiled in Table 1. Ten new resonances could be found in the present work. It has to be mentioned that it was not possible to fit the resonances at 4.325 and 12.35 keV with the gΓ_n values given in Ref.[9] since g$\Gamma_n > A_\gamma$ is required by definition.

2
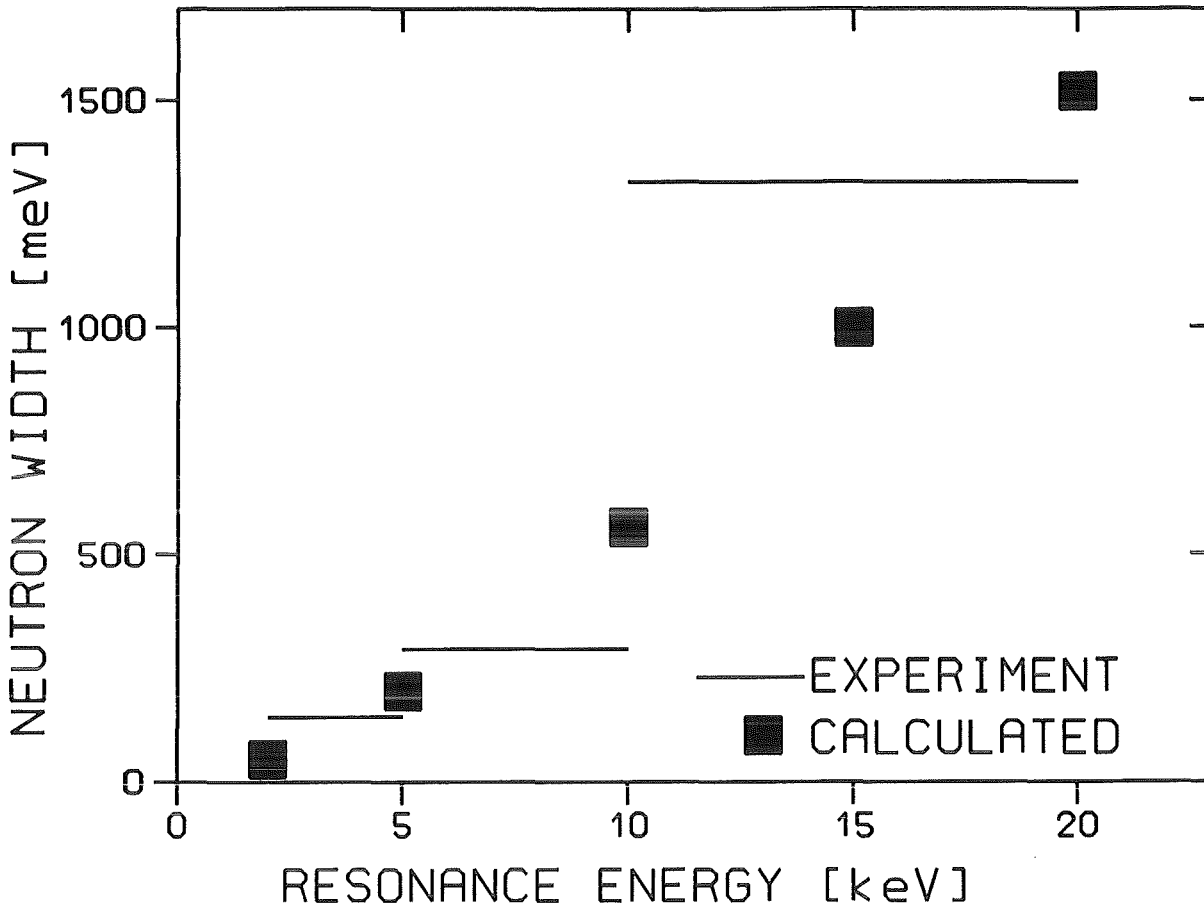
Figure 1: Comparison of the average neutron capture width of ^{120}Sn versus resonance energy between the experimental results of Ref.9 and the calculated values from Eq.(2).

The resonance energies are systematically lower compared to the data of Ref.[11] which were measured with significantly better energy resolution (17 m flightpath and 6 ns pulse width). The differences are linearly increasing with energy from 5 eV at 3 keV to 55 eV at 20 keV and are consistent with the flight path uncertainty of the present experiment.

In contrast to the example of ^{136}Ba [4] where the cross section is characterized by strong s–wave scattering resonances, the tin isotopes are located in a minimum of the s–wave strength function. Hence, the observed resonances exhibit small neutron widths which are well below 1000 meV at low energies. Therefore, the correction for multiple scattering, which is considered in the FANAC code, is typically 1 % , and less than 4 % for the resonances with the largest Γ_n.

The small neutron widths also exclude large systematic uncertainties for the capture area due to self–shielding effects. This has been demonstrated in Ref.[4] where it was shown that these uncertainties become compatible or larger than the statistical uncertainties only below 5 keV and gΓ_n–values above 1000 meV.

3

Table 1: Resonance areas of capture resonances in ^{120}Sn

Resonance energy		$g\Gamma_n$[1]	$g\Gamma_n\Gamma_\gamma/(\Gamma_n + \Gamma_\gamma)$	Uncertainty	Orbital angular momentum[1]
Ref.[9]	This Work				
(keV)	(keV)	(meV)	(meV)	(%)	
2.838	2.836	32	25.7	53	1
3.122	3.114	670	26.6	26	
3.290		2.9			
	3.620	120[3]	8.9	36	
	3.735	120[3]	6.4	45	
3.853	3.845	95	62.0	11.6	1
	4.100	150[3]	6.1	57	
	4.180[2]	150[3]	22.8	16.5	
4.200	4.210[2]	35	25.5	12.8	1
4.332	4.325[2]	40[4]	33.5	8.2	1
4.363	4.360[2]	400	22.8	26.4	0
	4.530	170[3]	7.9	42	
5.030	5.014	75	37.2	16.9	1
5.072	5.061	585	80.2	6.7	1
5.192	5.184	68	40.6	14.2	1
6.673	6.659	154	116.8	3.8	1
6.813		8			
6.823	6.808	55	3.4	80	
6.974	6.958	150	48.8	9.1	1
7.116	7.105	90	28.2	13.1	1
7.302	7.285	390	39.8	9.9	0
7.495	7.477	114	60.4	10.3	1
8.160	8.146	854	68.0	6.9	1
8.608	8.587[2]	115	88.0	6.3	1
8.664	8.643[2]	69	27.4	24	1
8.943	8.921	7650	28.9	21	0
9.117	9.099	53	48.0	7.9	1
9.543	9.534	1710	72.5	7.3	1
10.32	10.29	268	62.6	7.5	1
	10.53	570[3]	31.9	12.6	
10.88	10.85	650	105.4	4.3	1
11.28	11.25	833	93.8	4.6	1
11.48	11.45	303	79.2	12.9	0
11.66	11.63	150	66.6	9.0	1
11.79	11.76	597	44.6	11.4	0
12.35	12.30	70[4]	64.3	5.5	
12.68	12.65	48	27.3	26	
12.87	12.83	645	125.3	3.9	1
13.05	13.02	616	21.5	14.0	0
	13.75[2]	830[3]	34.9	15.4	
	13.85[2]	830[3]	32.8	16.7	

4

Table 1 (continued)

Resonance energy		$g\Gamma_n$[1]	$g\Gamma_n\Gamma_\gamma/(\Gamma_n + \Gamma_\gamma)$	Uncertainty	Orbital angular momentum[1]
Ref.[9] (keV)	This Work (keV)	(meV)	(meV)	(%)	
14.26	14.19	160	88.1	8.5	1
14.73	14.69	246	66.3	8.1	1
	15.10	1000[3]	32.5	13.2	
15.62	15.58	30	24.4	20	
16.14	16.10	5810	77.0	7.1	1
16.60	16.55	5150	160.8	4.1	1
16.71	16.66	261	15.9	29	1
17.17	17.11[2]	9760	173.3	4.3	1
17.31		103			
17.34	17.31[2]	430	134.7	5.2	1
17.43		114			
18.02	17.97[2]	965	23.1	12.2	0
18.23	18.15[2]	344	121.7	7.3	1
18.32	18.27[2]	57	34.4	21	
	18.74[2]	1380[3]	94.4	15.8	
19.00	18.95[2]	1420	26.9	23	(0)
19.30	19.22	2120	242.6	2.7	(0)
19.70	19.57	1480[3]	57.6	13.8	

[1]Taken from Ref.[9].
[2]Unresolved doublet.
[3]Calculated according to Eq.[2].
[4]Impossible to fit with $g\Gamma_n$ value given in Ref.[9].
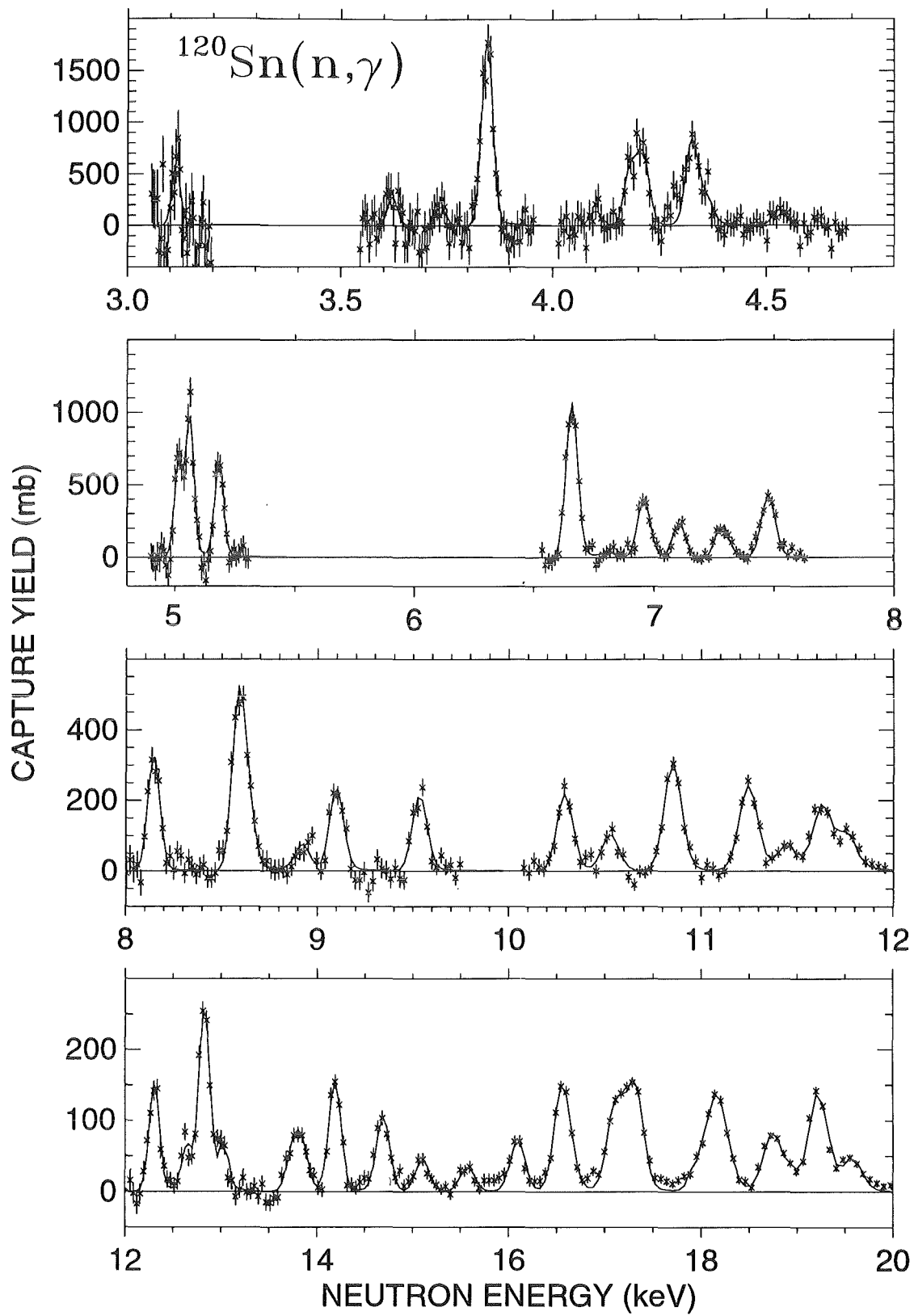
Figure 2: The neutron capture yield of ^{120}Sn and the corresponding FANAC fit .

The differences in A_γ for the two values of the spin factor g are in general below 1 %. Extreme differences of ± 2.5 % occurred for p–wave resonances with large Γ_n, for example at 16.14 and 16.6 keV, but even these are still negligible compared to the statistical uncertainties. Thus, systematic effects due to uncertainties of the input parameters can be excluded for ^{120}Sn. The quoted statistical uncertainties are those provided by the FANAC code. The experimental capture yields and the FANAC fit are compared in Fig. 2. The gaps in the data correspond to energy intervals without significant resonances.

- ^{118}Sn: In case of ^{118}Sn the situation is less favorable. Resonance energies and orbital angular momenta are available only for about half of the observed resonances, and neutron widths, Γ_n, are known for no more than four broad resonances below 5 keV (Adamchuk et al. [12]). The first two resonances were also observed by Fuketa et al. [13] who are reporting transmission spectra up to 10 keV. Presumably, the sensitivity of this measurement was not sufficient to observe the two other resonances at 3.9 and 4.7 keV, though at least the 4.7 keV resonance is fairly strong.

Therefore, Γ_n had to be calculated via Eq.(2) for most of the p–wave resonances. The energy dependence of Γ_n is the same as in Fig. 1 but the absolute values are scaled by a factor of 0.65 to account for the different level density and strength function. For s–wave resonances a constant average neutron width of 800 meV was assumed in the energy interval from 3 to 20 keV which was derived in the same way from the average 1455 meV of ^{120}Sn. Since there are very few s–wave resonances in the tin isotopes a reliable energy dependence could not be determined.

The resonance energies of this work and from a capture experiment by Raman et al. [14] are in good agreement below about 5 keV. For the other resonances listed in Ref.[9] a constant difference of 50 to 70 eV is observed which can hardly be explained by the experimental uncertainty.

The parameters of 67 resonances could be determined in the present measurement, 30 of these being reported for the first time (Table 2). The experimental capture yields and the respective FANAC fits are shown in Fig.3. The systematic uncertainties of the individual resonances are difficult to estimate with respect to the assumption on Γ_n but are probably sizable in some cases. However, below 5 keV where these uncertainties are largest the broad resonances are known and it is not likely that any resonance with $g\Gamma_n$ larger than 1000 meV could have been missed in the total cross section measurements [12, 13].

- ^{116}Sn: For this isotope only the energies and neutron widths of three broad resonances were known in the energy range from 3 to 20 keV [9, 12]. Therefore, all resonances were considered as p–waves and the neutron widths were calculated by means of Eq.(2). However, since data were recorded for two ^{116}Sn samples which differed by a factor of three in thickness [3], resonances with large Γ_n could be determined by their different self–absorption effects.

7

Table 2: Resonance areas of capture resonances in ^{118}Sn

Resonance energy Ref.[9] (keV)	This Work (keV)	$g\Gamma_n$[3] (meV)	$g\Gamma_n\Gamma_\gamma/(\Gamma_n+\Gamma_\gamma)$ (meV)	Uncertainty (%)	Orbital angular momentum[1]
2.889	2.902	65	29.7	17.8	(1)
2.976	2.966	1400[1]	46.2	13.4	
3.199	3.210	65	14.1	24	
3.460	3.439	1750[1]	35.7	19.8	
3.554	3.567	78	24.8	19.6	(1)
3.798	3.807	90	63.2	19.1	1
3.960	4.110	1100[1]	14.3	40	
4.248	4.258	103	30.1	18.6	
4.478	4.488	110	21.3	20	
4.592	4.600	116	50.5	12.1	
4.725	4.785	6300[1]	<12		0
4.920	4.928	130	104.2	7.1	1
5.071	5.077	130	40.3	13.4	1
	5.464	150	33.4	12.8	
	5.513	150	25.5	15.7	
5.616	5.667	162	123.7	4.7	
	5.981	175	11.5	31	
6.510	6.567	190	93.9	8.6	1
	6.702	200	60.9	8.7	
	6.979	220	65.1	8.6	
7.190	7.267	800[4]	46.9	14.9	0
	7.474	245	59.8	9.1	
	7.678	250	53.3	7.9	
	7.787	260	30.3	12.1	
8.160	8.224	270	149.3	6.2	1
8.540	8.597	300	78.2	8.0	1
	8.722	300	120.6	6.6	
	9.195	320	70.8	8.4	
	9.510	340	111.3	6.2	
9.590	9.659	340	67.6	7.9	
	9.866	350	91.6	6.5	
	10.01	350	44.2	11.9	
	10.15	360	61.1	9.6	
	10.43	390	64.0	8.7	
10.53	10.60	400	48.6	10.4	1
	10.85	410	24.7	19.2	
	10.97	420	34.9	15.3	
11.00	11.08	800[4]	55.2	12.6	0
11.20	11.26	430	98.1	6.3	1
11.51	11.57	450	111.5	5.4	
11.82	11.88	480	76.4	7.7	1

8

Table 2 (continued)

Resonance energy Ref.[9] (keV)	This Work (keV)	$g\Gamma_n$[3] (meV)	$g\Gamma_n\Gamma_\gamma/(\Gamma_n + \Gamma_\gamma)$ (meV)	Uncertainty (%)	Orbital angular momentum[1]
12.12	12.15	480	60.8	9.3	
12.41	12.46	800[4]	225.7	7.1	0
	12.71	520	44.6	11.0	
	13.00	550	14.7	35	
13.12	13.20	800[4]	265.6	7.6	0
13.48	13.55	800[4]	96.2	9.0	0
13.87	13.87	590	119.2	5.2	
	14.25	600	51.2	9.8	
	14.42	620	42.5	12.8	
14.70	14.77	640	144.1	4.9	
	15.03	645	76.0	10.9	
15.24	15.30	680	99.9	7.4	1
	15.51	680	58.5	12.9	
16.06	16.15	715	174.5	4.3	1
16.34	16.45	740	154.6	4.3	
16.86	16.94[2]	775	63.4	9.1	1
	17.12[2]	780	179.9	4.2	
	17.41	800	105.0	6.0	
17.65	17.76	820	188.7	3.5	1
	18.16[2]	840	82.2	12.0	
	18.32[2]	840	38.2	24	
18.65	18.73[2]	890	122.8	5.8	
	18.93[2]	900	78.0	9.2	
19.34	19.40[2]	930	58.3	9.7	
	19.65[2]	950	190.1	3.7	
	19.96	970	55.4	9.8	

[1]Taken from Ref.[9].
[2]Unresolved doublet.
[3]Calculated according to Eq.[2].
[4]For s–waves an average neutron width of 800 meV was assumed (see text).
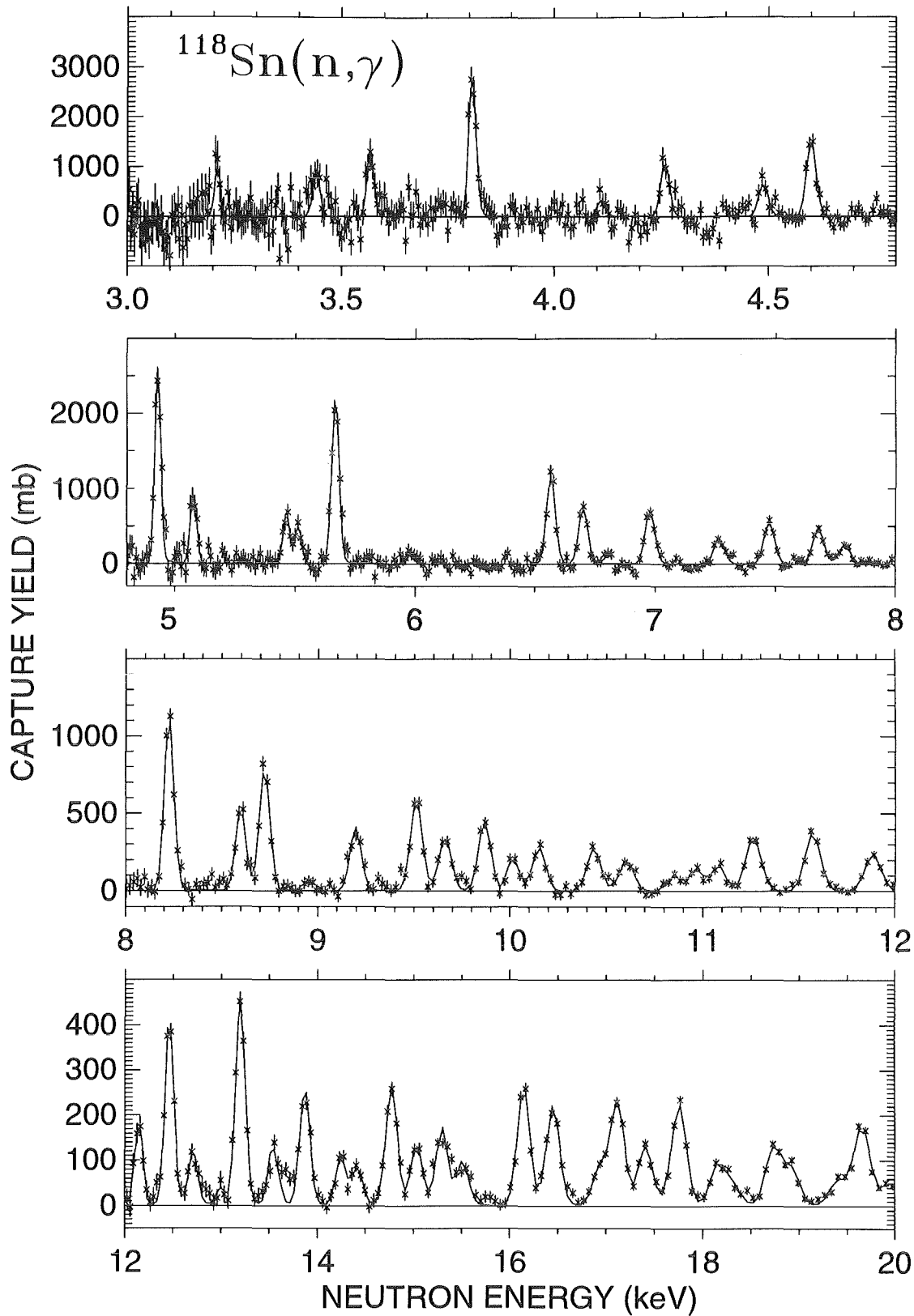
Figure 3: The neutron capture yield of ^{118}Sn and the corresponding FANAC fit .
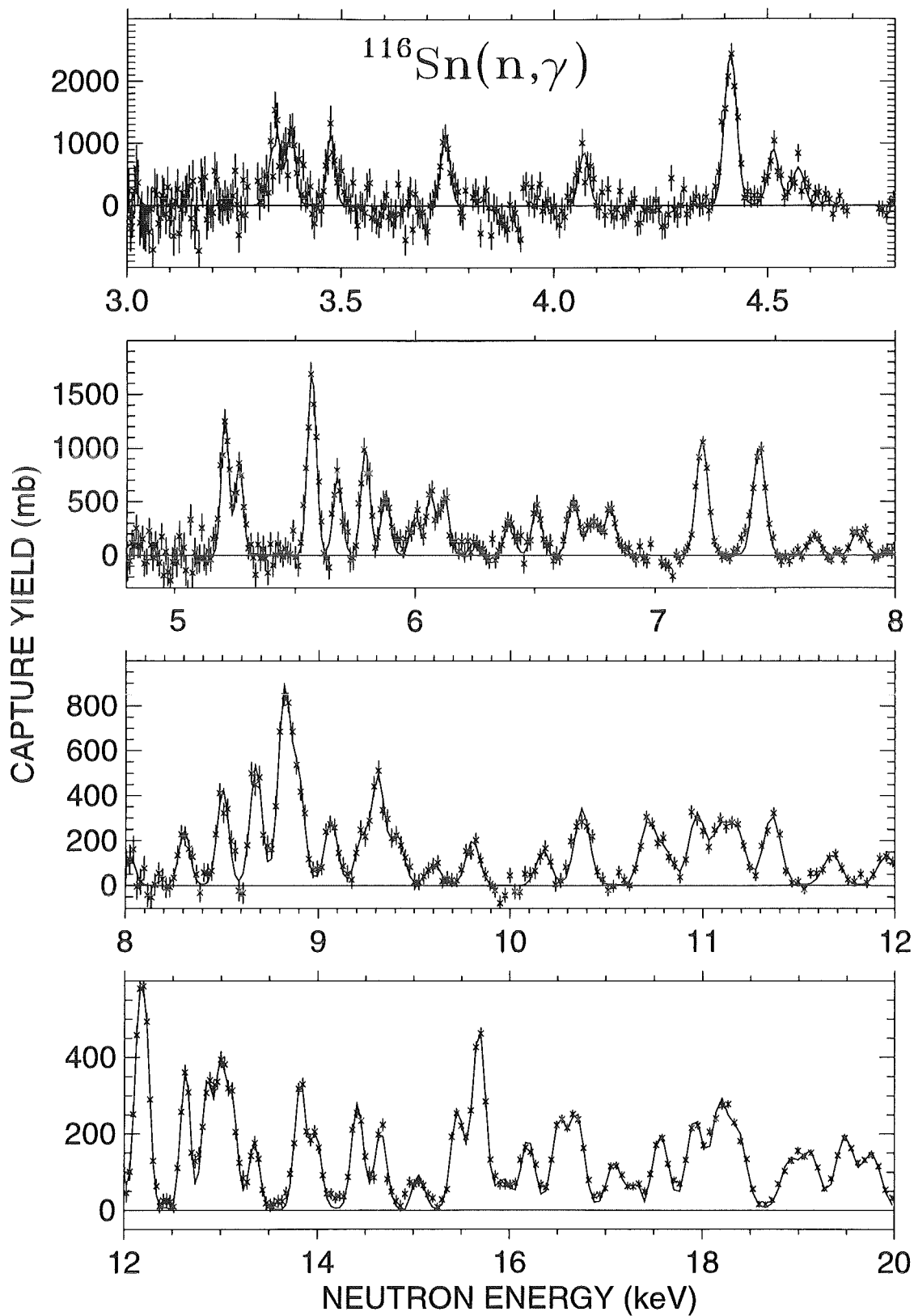
Figure 4: The neutron capture yield of ^{116}Sn measured with the thick sample and the corresponding FANAC fit .

Table 3: Resonance areas of capture resonances in ^{116}Sn

Resonance energy Ref.[9] (keV)	This Work (keV)	$g\Gamma_n{}^3$ (meV)	$g\Gamma_n\Gamma_\gamma/(\Gamma_n+\Gamma_\gamma)$ (meV)	Uncertainty (%)
	2.845	45	25.0	30.5
3.380	3.349	3900[1]	85.1	12.8
	3.384	48	25.8	25.5
3.460	3.476	1400[1]	53.4	14.8
	3.744	60	29.4	20.7
	4.070	65	26.5	28.2
4.640	4.414	4000[1]	297.6	4.3
	4.514	80	34.1	20.5
	4.572	84	24.0	21.4
	5.208	100	70.5	17.9
	5.267	100	46.5	15.1
	5.568	120	115.3	4.2
	5.676	110	47.4	18.1
	5.791	120	68.0	15.9
	5.876	120	40.6	15.6
	6.000	125	28.1	15.2
	6.064	126	42.1	13.0
	6.122	130	40.5	13.2
	6.248	130	9.4	35
	6.394	140	28.8	15.2
	6.508	140	39.3	14.5
	6.660	150	50.2	10.5
	6.740	150	33.1	13.3
	6.814	155	43.1	11.2
	7.194	160	122.3	14.4
	7.432	174	124.7	14.6
	7.660	180	22.8	20.4
	7.848	182	34.2	16.4
	8.023	190	18.5	36.8
	8.304	200	38.1	13.9
	8.504	200	69.0	10.4
	8.676	220	91.7	10.5
	8.821[2]	186	151.7	5.7
	8.895[2]	220	82.5	12.2
	9.066	230	54.3	11.2
	9.225[2]	230	40.1	19.1
	9.310[2]	240	96.6	11.5
	9.411	240	44.8	16.0
	9.602	250	20.1	26
	9.804	250	45.3	12.5
	10.17	260	37.8	18.0
	10.37	260	87.6	9.5
	10.71[2]	280	76.9	12.2

Table 3 (continued)

Resonance energy Ref.[9] (keV)	This Work (keV)	$g\Gamma_n$[3] (meV)	$g\Gamma_n\Gamma_\gamma/(\Gamma_n + \Gamma_\gamma)$ (meV)	Uncertainty (%)
	10.81[2]	280	40.1	19.7
	10.97	280	91.5	10.6
	11.09[2]	300	71.7	17.1
	11.18[2]	300	69.6	17.3
	11.36	300	97.5	7.9
	11.67	325	46.5	13.1
	11.96	340	47.7	14.4
	12.15[2]	320	166.3	19.8
	12.23[2]	320	144.0	20.2
	12.63	370	150.2	5.4
	12.86	370	140.1	7.3
	13.00[2]	390	159.8	8.1
	13.12[2]	390	119.9	9.5
	13.35	400	79.2	8.6
	13.82	400	167.2	5.6
	13.99	430	98.2	7.5
	14.42	440	155.2	5.7
	14.66	460	117.7	6.9
	15.05	470	56.1	10.7
	15.46	490	169.6	4.7
	15.68	529	320.7	3.6
	15.94	500	53.4	12.3
	16.19	520	133.1	6.0
	16.52	540	176.2	5.3
	16.70	540	188.7	5.1
	17.09	570	101.3	6.6
	17.32	600	56.7	12.4
	17.57	590	176.7	4.7
	17.92	600	219.0	4.8
	18.18[2]	620	259.2	5.5
	18.37[2]	640	187.7	6.0
	18.91[2]	660	134.2	6.4
	19.12[2]	660	158.8	5.8
	19.48	690	218.3	4.0
	19.76	700	172.2	4.5

[1]Taken from Ref.[9].
[2]Unresolved doublet.
[3]Calculated according to Eq.[2].
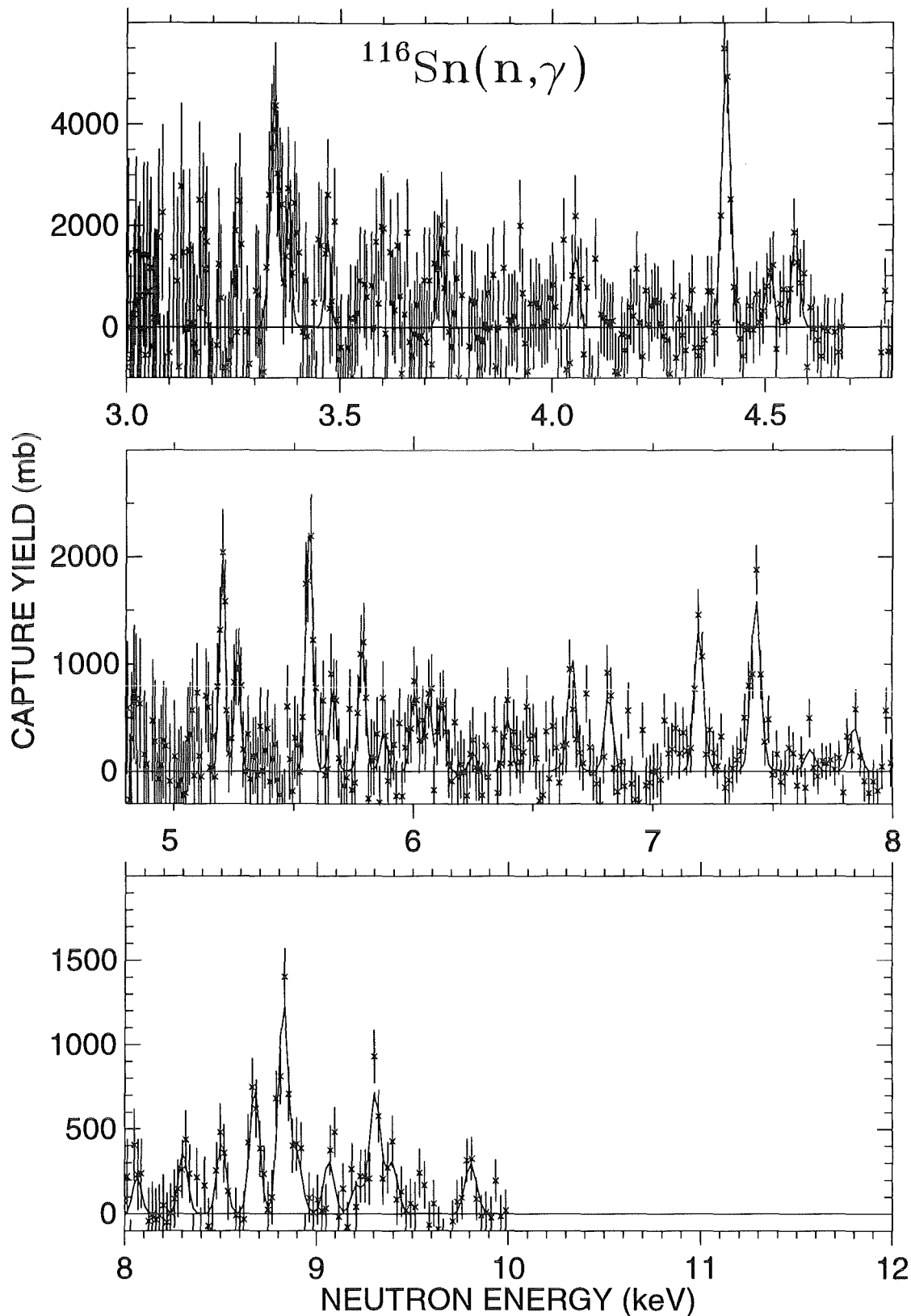
Figure 5: The neutron capture yield of ^{116}Sn measured with the thin sample and the corresponding FANAC fit .

In a first step all resonances were analyzed with the calculated neutron widths. For most resonances the resulting values of A_γ agreed for both samples within the statistical uncertainties. The only exceptions were two strong resonances at 3.349 keV and 4.414 keV and a weak resonance at 6.00 keV. In these cases the result from the thin sample was up to two times larger, indicating a large neutron width. The resonance at 3.349 keV can easily be assigned to the resonance at 3.380 ± 0.015 keV reported by Adamchuk *et al.* [12]. The resonance at 4.414 keV was assumed to correspond to the 4.640 keV resonance in Ref. [12] though the energy difference is far outside the quoted uncertainties. Since the resonance at 6.00 keV is very weak the observed difference in the fitted area should only be taken as a hint for a large neutron width.

The final resonance energies and areas of 78 resonances are given in Table 3. The capture yield of both samples is shown together with the FANAC fit in Figs. 4 and 5. This comparison demonstrates that the better energy resolution obtained with the thin sample can not compensate for the poorer statistics in most cases.

As for the other isotopes the systematic uncertainties are large for low energy resonances if the true neutron width is significantly larger than the value used in the fit. The measurement with the two samples can exclude this problem only for resonances with large A_γ.

It has to be emphasized that the present experiment was not optimized for the determination of resonance parameters, and can not compete in this respect with LINAC measurements using much longer flight paths. As indicated in Tables 1 to 3 several resonances were not completely resolved. In these cases, the sum of both resonances should always be used for comparison with other data. For the accurate determination of average cross sections which was the main purpose of the present experiment this split of the capture strength in a resonance doublet is not important.

3 Results

Average capture cross sections were calculated from the resonance parameters listed in Tables 1 to 3. The comparison with the previous analysis [3] in Table 4 shows satisfactory agreement within the statistical uncertainties, thus confirming the proper treatment of the background due to scattered neutrons which is comparably large at low energies. Only for two entries (^{116}Sn, 3-5 keV and ^{118}Sn, 7.5-10 keV) the difference exceeds the 2σ level. However, there is a systematic trend, the new results being lower on average by 6 % (^{118}Sn and ^{120}Sn) to 8 % (^{116}Sn). This difference may be due to several reasons:

- As mentioned before, the resonance areas are underestimated if too small neutron widths were used in the analysis. This possibility can be excluded since the difference occurs also for ^{120}Sn where the Γ_n are known for most resonances, and because the effect does not show the corresponding energy dependence which would prefer the lower energies.

Table 4: Averaged capture cross section of ^{116}Sn, ^{118}Sn, and ^{120}Sn.

Neutron energy (keV)	Capture cross section (mb)[1]					
	^{116}Sn		^{118}Sn		^{120}Sn	
	This Work	Ref.[3]	This Work	Ref.[3]	This Work	Ref.[3]
3–5	297.5 ± 12.8	205.0 ± 17.	181.0 ± 10.9	217.5 ± 19.	117.4 ± 8.0	113.1 ± 16.
5–7.5	254.6 ± 9.5	293.5 ± 8.5	149.1 ± 4.7	157.4 ± 8.3	122.3 ± 4.1	135.6 ± 7.1
7.5–10	152.4 ± 5.3	168.7 ± 5.1	145.8 ± 3.6	175.1 ± 5.4	62.9 ± 2.5	73.8 ± 4.4
10–12.5	143.3 ± 7.4	156.5 ± 3.4	132.3 ± 3.6	120.1 ± 3.5	81.0 ± 2.3	80.2 ± 2.8
12.5–15	146.6 ± 3.5	156.7 ± 2.8	94.4 ± 3.2	96.6 ± 2.6	48.4 ± 1.8	57.4 ± 2.1
15–20	133.1 ± 1.8	138.2 ± 1.5	82.6 ± 1.4	86.4 ± 1.4	57.2 ± 1.3	59.3 ± 1.1

[1]Including statistical uncertainty

Table 5: Maxwellian averaged neutron capture cross sections of ^{116}Sn, ^{118}Sn, and ^{120}Sn.

Thermal energy kT (keV)	$< \sigma v > / v_T$ (mb)[1]					
	^{116}Sn		^{118}Sn		^{120}Sn	
	This Work	Ref.[3]	This Work	Ref.[3]	This Work	Ref.[3]
10	168.6 ± 2.6	171.6 ± 2.6	121.0 ± 3.1	126.6 ± 3.1	69.9 ± 1.7	73.2 ± 1.7
12	152.6 ± 2.1	155.4 ± 2.1	108.0 ± 2.3	112.4 ± 2.3	62.4 ± 1.3	65.1 ± 1.3
20	114.3 ± 1.3	116.1 ± 1.3	78.2 ± 1.1	80.3 ± 1.1	45.3 ± 0.7	46.7 ± 0.7
25	100.7 ± 1.1	102.1 ± 1.1	68.3 ± 0.8	69.7 ± 0.8	39.5 ± 0.6	40.5 ± 0.6
30	90.9 ± 0.9	91.9 ± 0.9	61.6 ± 0.6	62.6 ± 0.6	35.7 ± 0.5	36.4 ± 0.5

[1]With total uncertainty except for the 1.5% systematic uncertainty of the gold cross section.

- Weak resonances are likely to be missed in the fit. Closer inspection of Figs. 2 to 5 shows that there are certainly some possibilities for such resonances which are obscured by the counting statistics.

- Nonresonant direct capture may yield a nonnegligible contribution to the relatively small cross sections of the even tin isotopes.

Based on the results of Table 4 revised Maxwellian averaged cross sections for kT values from 10 to 30 keV are given in Table 5 together with the previous results. Despite of the uncertainties of the resonance analyses it is important to note that there are only marginal differences between the two data sets which are completely accounted for by the quoted uncertainties.

4 Conclusions

The improved analysis of the neutron capture cross sections of ^{116}Sn, ^{118}Sn, and ^{120}Sn in the energy range from 2.8 to 20 keV yielded the resonance areas of 78, 67, and 55 resonances, respectively. The resulting averaged cross sections are in good agreement with a first analysis which was based on the observed capture yields only [3]. This good agreement provides an additional confirmation for the reliability of background subtraction in experiments with the Karlsruhe 4π BaF$_2$ detector. The Maxwellian averaged cross sections could be slightly improved for low kT values but remain essentially unchanged. Therefore, previous results of s–process studies based on these cross sections [3] are not affected.

5 Acknowledgments

References

[1] Zs. Németh, T. Belgya, S.W. Yates, Ch. Theis, and F. Käppeler, Proc. 2nd International Symposium Nuclei in the Cosmos, Eds. F. Käppeler and K. Wisshak, Karlsruhe Germany 6–10 July 1992, IOP Publishing, Bristol and Philadelphia (1993) p219.

[2] Zs. Németh, F. Käppeler, Ch. Theis, T. Belgya, and S.W. Yates, Astrophys. J. **426**, 357 (1994).

[3] K. Wisshak, F. Voss, Ch. Theis, F. Käppeler, K. Guber, L. Kazakov, N. Kornilov, and G. Reffo, report FZKA–5603, Forschungszentrum Karlsruhe (1995) and Phys. Rev. C submitted for publication.

[4] F. Voss, K. Wisshak, and F. Käppeler, Phys. Rev. C **52**, 1102 (1995).

[5] F. Käppeler, R. Gallino, M. Busso, G. Picchio, and C. Raiteri, Astrophys. J. **354**, 630 (1990).

[6] O. Straniero, R. Gallino, M. Busso, A. Chieffi, C. Raiteri, M. Limongi, and M. Salaris, Astrophys. J. **440**, L85 (1995).

[7] K. Wisshak, K. Guber, F. Käppeler, J. Krisch, H. Müller, G. Rupp, and F. Voss, Nucl. Instrum. Meth. Ser. A **292**, 595 (1990).

[8] F. H. Fröhner, report KfK–2145, Kernforschungszentrum Karlsruhe (1977).

[9] S.F. Mughabghab, M. Divadeenam, and N.E. Holden, Neutron Cross Sections Vol 1. Part A, Academic Press, New York (1984).

[10] F. H. Fröhner, report GA–8380, Gulf General Atomic, 1968.

[11] R.F. Carlton, S. Raman, J.A. Harvey, and G.G. Slaughter, Phys. Rev. C **14**, 1439 (1976).

[12] Yu.V. Adamchuk, S.S. Moskalev, and G.V. Muradyan, Sov. J. Nucl. Sci. **3**, 589 (1966).

[13] T. Fuketa, F.A. Khan, and J.A. Harvey, Report ORNL–3425, Oak Ridge National Laboratory, 1963.

[14] S. Raman, R.F. Carlton, G.G. Slaughter, and M.R. Meder, Phys. Rev. C **18**, 1158 (1978).